Cellular and Molecular Life Sciences

ORIGINAL ARTICLE

CrossMark

RECK (reversion-inducing cysteine-rich protein with Kazal motifs) regulates migration, differentiation and Wnt/β-catenin signaling in human mesenchymal stem cells

Christian Mahl[1] · Virginia Egea[1] · Remco T. A. Megens[1,2] · Thomas Pitsch[1] ·
Donato Santovito[1] · Christian Weber[1,2,3] · Christian Ries[1]

Abstract The membrane-anchored glycoprotein RECK (reversion-inducing cysteine-rich protein with Kazal motifs) inhibits expression and activity of certain matrix metalloproteinases (MMPs), thereby suppressing tumor cell metastasis. However, RECK's role in physiological cell function is largely unknown. Human mesenchymal stem cells (hMSCs) are able to differentiate into various cell types and represent promising tools in multiple clinical applications including the regeneration of injured tissues by endogenous or transplanted hMSCs. RNA interference of RECK in hMSCs revealed that endogenous RECK suppresses the transcription and biosynthesis of tissue inhibitor of metalloproteinases (TIMP)-2 but does not influence the expression of MMP-2, MMP-9, membrane type (MT)1-MMP and TIMP-1 in these cells. Knockdown of RECK in hMSCs promoted monolayer regeneration and chemotactic migration of hMSCs, as demonstrated by scratch wound and chemotaxis assay analyses. Moreover, expression of endogenous RECK was upregulated upon osteogenic differentiation and diminished after adipogenic differentiation of hMSCs. RECK depletion in hMSCs reduced their capacity to differentiate into the osteogenic lineage whereas adipogenesis was increased, demonstrating that RECK functions as a master switch between both pathways. Furthermore, knockdown of RECK in hMSCs attenuated the Wnt/β-catenin signaling pathway as indicated by reduced stability and impaired transcriptional activity of β-catenin. The latter was determined by analysis of the β-catenin target genes Dickkopf1 (*DKK1*), axis inhibition protein 2 (*AXIN2*), runt-related transcription factor 2 (*RUNX2*) and a luciferase-based β-catenin-activated reporter (BAR) assay. Our findings demonstrate that RECK is a regulator of hMSC functions suggesting that modulation of RECK may improve the development of hMSC-based therapeutical approaches in regenerative medicine.

Keywords RECK · hMSC · Chemotactic migration · Osteogenic differentiation · Canonical Wnt/β-catenin signaling

Abbreviations

ALP	Alkaline phosphatase
AXIN2	Axis inhibition protein 2
BAR	β-Catenin-activated reporter
COM	Displacement of the center of mass
DKK1	Dickkopf1
ECM	Extracellular matrix
FMI	Forward migration index
GAPDH	Glyceraldehyde-3-phosphate dehydrogenase
hMSC	Human mesenchymal stem cell
LEF	Lymphoid enhancer factor
MMP	Matrix metalloproteinase
MSCGM	Mesenchymal stem cell growth medium
MT1-MMP	Membrane-type 1 matrix metalloproteinase
PPARγ	Peroxisome proliferator-activated receptor γ
qRT-PCR	Quantitative real-time polymerase chain reaction

✉ Christian Ries
christian.ries@med.uni-muenchen.de

1 Institute for Cardiovascular Prevention, Ludwig-Maximilians-University of Munich, Pettenkoferstrasse 9b, 80336 Munich, Germany

2 Cardiovascular Research Institute Maastricht, Maastricht University, Maastricht, The Netherlands

3 German Centre for Cardiovascular Research, Partner Site Munich Heart Alliance, Munich, Germany

RECK	Reversion-inducing cysteine-rich protein with Kazal motifs
RUNX2	Runt-related transcription factor 2
siRNA	Small interfering RNA
TCF	T cell factor
TIMP	Tissue inhibitor of metalloproteinase
Wnt	Wingless-type mouse mammary tumor virus integration site

Introduction

HMSCs from bone marrow are nonhematopoietic adult stem/progenitor cell-like cells also referred to as multipotent mesenchymal stromal cells [1]. hMSCs are characterized by their ability to differentiate into osteocytes, adipocytes and chondrocytes [2] as well as other mesodermal and non-mesodermal cell types such as neural [3] and endoderm-like cells [4]. Furthermore, these cells have the capacity for self renewal [5], directed migration [6] and the release of immunosuppressive cytokines [7]. As a consequence, hMSCs represent a powerful cell-based therapeutic option for tissue regeneration in several pathological conditions including bone loss [8], myocardial infarction [9] and neurodegenerative disorders [10]. Moreover, the immuno-modulatory potential of these cells features a valuable tool for clinical applications dealing with autoimmune diseases [11], transplantations [12] or injured tissues [13].

In order to reach sites of tissue repair and inflammation, hMSCs need to migrate through barriers of extracellular matrix (ECM) including basement membranes. This is accomplished by surface expression or secretion of ECM-degrading proteinases such as MMP-1, MMP-2, MMP-9 and MT1-MMP, as previously demonstrated by own studies and those of others [14–17]. Once activated, MMPs are primarily modulated by their specific binding to TIMPs. TIMP-1 and TIMP-2 preferentially interact with MMP-9 and MMP-2, respectively [18]. Activation of proMMP-2 is achieved by a unique mechanism involving TIMP-2, MT1-MMP and proMMP-2 forming a trimolecular complex on the cell surface [19].

Wnt ligands represent another class of hMSC-secreted regulatory proteins [20]. Specific (co-)receptor binding of Wnts activates the canonical Wnt/β-catenin pathway, a signaling cascade that is crucial for differentiation [21] as well as proliferation and directed migration [22] of hMSCs. After interaction of Wnts with heterodimers of frizzled class receptors (FZDs) and low density lipoprotein receptor-related proteins (LRPs) on the cell surface, cytoplasmic β-catenin is prevented from glycogen synthase kinase 3 β (GSK3β)-mediated phosphorylation and subsequent degradation by the proteasome. This enables β-catenin to translocate into the nucleus [23]. Here, it interacts with the transcription factors T cell factor (TCF) [24] and lymphoid enhancer factor (LEF) [25], resulting in the transcription of several target genes such as *DKK1* [26], *AXIN2* [27] and *RUNX2* [28].

The C-terminal glycosylphosphatidylinositol (GPI)-anchored glycoprotein RECK [29] is a potent inhibitor of MMP-2, MMP-9 and MT1-MMP on both transcriptional [30] and posttranscriptional [31, 32] level. RECK participates in ECM remodeling during embryogenesis [31] and carcinogenesis [33] due to MMP regulation in vivo. For instance, RECK affects MMP-9-mediated bioavailability of vascular endothelial growth factor (VEGF) thus impairing angiogenesis in a pancreatic cancer mouse model [34]. RECK is ubiquitously expressed in normal human tissues and organs including brain, heart and thymus [29]. However, basal RECK expression is significantly reduced in various malignant tumors of the lung [35], breast [36], skin [37] and other organs, making RECK a reliable tumor prognosis marker [33].

Up till now, research on RECK was mainly focused on its importance in cancer. In this study, we investigated the role of RECK in non-malignant cells with emphasis on essential stem/progenitor cell functions such as migration, proliferation and differentiation. Our results indicate that RECK is a promoter of hMSC migration by mechanisms different from tumor cells, a reciprocal regulator of adipogenic and osteogenic differentiation and a positive effector of canonical Wnt/β-catenin signaling in these cells.

Materials and methods

Cultivation, differentiation and histochemical staining of hMSCs

Bone marrow-derived hMSCs were purchased from Lonza (Basel, Switzerland). The cells were tested for purity by flow cytometry analysis and differentiation capacity into adipogenic, osteogenic and chondrogenic lineages. The cells were positive for cluster of differentiation (CD)29, CD44, CD105, CD166 and negative for CD14, CD34, CD45.

hMSCs were cultivated as previously described [14], using the mesenchymal stem cell growth medium (MSCGM) Bullet Kit (Lonza) and StemMACS mesenchymal stem cell medium (Miltenyi Biotec, Bergisch Gladbach, Germany). Serum-free cultivation was carried out by incubation in RPMI-1640 (GE Healthcare, Little Chalfont, United Kingdom) supplemented with 1 % Nutridoma SP (Roche, Basel, Switzerland) in the presence or absence of 100 ng/mL murine recombinant Wnt3a

(Peprotech, Rocky Hill, NJ, USA). All experiments were carried out with hMSCs of a passage between 4 and 6.

Adipogenic and osteogenic differentiation of hMSCs as well as Oil Red O and Alizarin Red S staining were conducted as previously described [38]. Oil Red O and Alizarin Red S incorporation was quantified by extracting stained monolayers with a solution containing 50 % ethanol as well as 10 % SDS and a buffer (10 mM Na_2HPO_4, pH 7.0) containing 10 % (w/v) cetylpyridinium chloride, respectively. Aliquots of the extracted dye were then transferred to 96-well plates and the absorbance at 405 nm (for Oil Red O) and 550 nm (for Alizarin Red S) was determined by use of an ELISA reader (Mikrotek, Overath, Germany).

Quantification of cell proliferation and metabolic activity

Cell proliferation was quantified using the CyQuant cell proliferation assay kit (Invitrogen, Carlsbad, CA, USA) according to the manufacturer's protocol. This method is based on staining of DNA with the fluorescent dye CyQuant GR and subsequent detection at 480 nm (excitation) and 530 nm (emission). For each experiment, a standard calibration curve was generated by plotting the samples fluorescence values versus the respective cell number that had been determined before staining by use of a hemocytometer.

The Cell Counting Kit-8 (Dojindo, Rockville, MD, USA), that is based on the cleavage of the tetrazolium salt WST-8 by mitochondrial dehydrogenases in viable cells, was used following the instructions of the manufacturer.

Transfection of hMSCs with small interfering RNA (siRNA)

Specific knockdown of RECK in hMSCs was accomplished by application of RNA interference technology. Considering the guidelines of Reynolds et al. [39], siRNA sense and antisense oligonucleotides targeting human RECK were designed in our laboratory. RECK siRNA 1 (sense sequence: AAAUUAUUGCGCCUCUAUUTT, antisense sequence: AAUAGAGGCGCAAUAAUUUTC) was synthesized by Qiagen (Hilden, Germany), while RECK siRNA 2 (sense sequence: AAUAGAGGCGCAAUAAUUUCCCCC, antisense sequence: GGGGGAAAUUAUUGCGCCUCUAUU) was provided by Riboxx (Radebeul, Germany). The latter contains a GC-clamp at its 3′ end for increased stability against degradation [40] and reduced off-target effects [41]. β-catenin siRNA (sense sequence: UGGUUGCCUUGCUCAA-CAATT, antisense sequence: UUGUUGAGCAAGGCAAC CATT) was produced by Qiagen. A non-specific siRNA with no target in the human transcriptome (AllStars Negative

Control siRNA, sense sequence: UUCUCCGAACGUGU-CACGU, antisense sequence: ACGUGACACGUUCGGAG AA) was used as a negative control (Qiagen). hMSCs were transfected with the siRNAs as previously described [38] with some modifications. Briefly, 1×10^5 cells were transferred into a well of a 6-well plate and grown until subconfluency. Then the cultivation medium was replaced by 750 μL of fresh MSCGM (Lonza). Subsequently, the transfection mix was added to the cells. It contained 250 μL RPMI-1640 (GE Healthcare), 2 % Lipofectamine 2000 (Invitrogen), 1 % Nutridoma SP (Roche) and siRNA in a final concentration of 50 nM.

Transcription-based reporter assay of Wnt/β-catenin signaling

To monitor the activity of the Wnt/β-catenin signaling pathway characterized by TCF/LEF-dependent target gene transcription, we deployed a modified reporter assay as previously described in detail [42]. Briefly, we used the BAR that contains multimerized TCF/LEF DNA-binding sites [43] and modified it by cloning *Gaussia* luciferase as the reporter gene to allow the detection of the reporter in the conditioned medium without lysing the cells. After hMSCs were transfected with the BAR *Gaussia* luciferase reporter plasmid, the cells were cultivated for the indicated time intervals and analyzed for the presence of reporter protein in the culture supernatants using the *Gaussia* luciferase assay kit (New England Biolabs, Ipswich, MA, USA) following the manufacturer's instructions. Sample luminescence was quantified using a plate-reading luminometer (Tecan, Maennedorf, Switzerland).

Quantitative real-time polymerase chain reaction (qRT-PCR)

RNA isolation, cDNA synthesis and PCR were performed as specified [14]. qRT-PCR was conducted on a LightCycler (Roche) using the LightCycler FastStart DNA Master SYBR Green I Kit (Roche). For mRNA quantification of RECK, MMP-2, MMP-9, MT1-MMP, TIMP-1, TIMP-2, peroxisome proliferator-activated receptor γ (PPARγ), alkaline phosphatase (ALP), DKK1, AXIN2, RUNX2, β-catenin and the house-keeping gene standard glyceraldehyde-3-phosphate dehydrogenase (GAPDH), LightCycler Primer Sets (Search-LC, Heidelberg, Germany) were applied according to the manufacturer's instructions.

Western blot analysis

hMSC lysis and protein extraction were accomplished by use of a buffer containing 40 mM Tris–HCl pH 8.0, 150 mM NaCl, 1 % NP-40, 0.5 % sodium deoxycholate,

0.1 % SDS and a mixture of proteinase and phosphatase inhibitors (cOmplete Mini Tablets and PhosSTOP; Roche). SDS-PAGE was performed under reducing conditions in precast 4–12 % mini-gels (Invitrogen). After protein transfer, Immobilon PVDF Transfer Membranes (Millipore, Billerica, MA, USA) were incubated with monoclonal antibodies against RECK (1:500; BD Biosciences, San Jose, CA, USA), TIMP-1 (1:500; Abcam, Cambridge, UK), TIMP-2 (1:500; R&D systems, Minneapolis, MN, USA), β-catenin (1:1000; Cell Signaling Technology, Danvers, MA, USA) and PPARγ (1:1000; Thermo Fisher Scientific, Waltham, MA, USA) as well as polyclonal antibodies against MT1-MMP (1:2000; Chemicon, Temecula, CA, USA) and the house-keeping gene standard β-actin (1:1,000,000; Abcam), diluted in Tris-buffered saline containing 0.1 % Tween-20 (TBS-Tween buffer) without or with (for TIMP-2 detection) 10 % Blocking agent (Amersham, Amersham, UK) at 4 °C overnight. After washing the membranes with TBS-Tween buffer, peroxidase-conjugated anti-rabbit IgG (β-catenin, PPARγ, MT1-MMP, β-actin) or anti mouse IgG (RECK, TIMP-1) (both from Cell Signaling Technology) were applied at a dilution of 1:2000 in TBS-Tween for 30 min. For TIMP-2 we used peroxidase-conjugated anti-mouse IgG (DakoCytomation, Carpinteria, CA, USA) diluted at 1:4000 in TBS-Tween for 15 min. Bound antibodies were detected via the enhanced chemiluminescence system (GE Healthcare). Recombinant protein standards (Invitrogen) were applied for molecular mass determination. Densitometric quantification of developed films was performed using a GS-800 Calibrated Densitometer driven by Quantity One 1-D Analysis software (Bio-Rad Laboratories, Hercules, CA, USA) as recommended by the distributor.

Zymography analysis

Zymography analysis was carried out as described previously [44]. Briefly, samples were run under non-reducing conditions without prior boiling in precast 10 % polyacrylamide mini-gels containing 0.1 % gelatin as substrate (Invitrogen). After electrophoresis, gels were washed twice for 15 min in 2.7 % Triton X-100 on a rotary shaker to remove SDS and to allow proteins to renature. The gels were then incubated in a buffer containing 50 mM Tris–HCl pH 7.5, 200 mM NaCl, 5 mM $CaCl_2$ and 0.2 % Brij35 (Invitrogen) for 18 h at 37 °C. The zymograms were stained for 90 min with 0.02 % Coomassie Blue R-350 in a 30 % methanol/10 % acetic acid solution using PhastGel-Blue-R tablets (GE Healthcare). Areas of substrate digestion appear as clear bands against a darkly stained background. Densitometric quantification of developed zymograms was performed as described for Western blots.

Scratch wound assay and microscopic analysis

Carrying out a modified protocol of Lipton et al. [45], hMSCs were grown in a 6-well plate until confluency and set serum-free before being assayed. The monolayers of both control and RECK knockdown cells were subsequently scratched using a 200 μL pipette tip.

The plate was then incubated in an Axiovert S100 microscope equipped with an AxioCam ICc3 camera (Carl Zeiss, Oberkochen, Germany) at 37 °C and 5 % CO_2. Images were acquired every 24 h for 3 days and analyzed using ImageJ software (NIH, Bethesda, MD, USA) including an algorithm for determination of cell density [46]. Wound closure was defined as the relative increase of area covered by cell bodies.

μ-Slide Chemotaxis3D assay and life cell imaging analysis

Studies on directed migration of hMSCs were performed using the μ-Slide Chemotaxis3D assay (Ibidi, Martinsried, Germany) following the manufacturer's recommendations. The μ-Slides allow time-lapse microscopy analysis of adherent cells in a narrow observation area between two large reservoirs that constitute gradients of chemoattractants. HMSCs were trypsinized and resuspended in serum-free medium at a final concentration of 1.25×10^6 cells/mL. After placing a total of 7.5×10^3 cells into the observation channel of a μ-Slide, both medium reservoirs were filled with 65 μL RPMI-1640 (GE Healthcare) supplemented with 1 % Nutridoma SP (Roche). Three days of cultivation allowed attachment of hMSCs and full recovery of RECK expression on the cell surface. The experiments were started by adding 10 % human serum (PAA Laboratories, Pasching, Austria) as a mixture of chemoattractants to one medium reservoir.

The μ-Slide was then incubated for 24 h at 37 °C in an IX70 microscope (Olympus, Tokyo, Japan) that was connected to a SensiCam camera (PCO Imaging, Kelheim, Germany). Serial images of cell movement from a total of 30 hMSCs in each observation channel were captured by taking pictures every 20 min. The resulting images were converted to a stack using the ImageJ software (NIH). To determine the migration path of hMSCs, the image stacks were analyzed by deploying the Manual Tracking plug-in as well as the Chemotaxis and Migration Tool (both from Ibidi) following the recommendations of the provider.

To quantify and characterize effects on both chemotactic and migratory potential of hMSCs, several parameters were determined. The chemotactic potential of a distinct cell population is judged from the values obtained by assessment of the Rayleigh test, the moving direction and the forward migration index (FMI). The Rayleigh test

statistically determines the uniformity of initially circular distributed cells, indicating inhomogeneity at the end of the experiment with a probability value <0.05 [47]. The moving direction indicates migration towards or away from the chemoattractant, depending on the final position of a cell. The FMI quantifies the directness of cell movements and represents the ratio between the Euclidean distance of a cell and its migration distance. The Euclidean distance is defined as the shortest distance between the initial and the final position. In our experiments, the chemotactic gradient is located along the y-axis, meaning that FMI (y) values >0 highlight positive chemotaxis with a maximum of 1. The migratory potential of a distinct cell population is characterized by the parameters displacement of the center of mass (COM), migration distance and velocity. The COM represents the location of the cell population center relative to its initial position being equal to the mean Euclidean distance of all traced cells. The migration distance displays the summary of all cell center movements between images. The velocity indicates the mean migration distances of a cell population over time.

Statistical analysis

Statistics were calculated using SPSS Statistics version 20.0 (IBM Corporation, Armonk, NY, USA). Values are reported as mean value and standard deviation. The Levene test was used to assess variance homogeneity. Comparisons between two groups were evaluated by a 2-sample t test with Welch correction as appropriate. For three or more groups, standard 1-way ANOVA followed by Bonferroni post hoc test or the Brown-Forsythe test followed by Games-Howell post hoc test were performed according variance homogeneity. Factorial-ANOVA with Bonferroni post hoc test was used to analyze data from the scratch assay. A 2-tailed probability value <0.05 was deemed as statistically significant.

Results

Effects of RECK on MMP and TIMP expression in hMSCs

For knockdown of endogenous RECK expression in hMSCs, we applied RNA interference technology using two different siRNAs directed against RECK, siRNA 1 and siRNA 2 with the latter containing a stabilizing guanine-cytosine base clamp. hMSCs transfected with siRNAs targeting RECK demonstrated dramatically reduced levels of RECK mRNA and protein on day 1–10 and day 3–14 after transfection, respectively, in comparison to cells treated with a non-specific control siRNA as determined by

qRT-PCR (Fig. 1a) and Western blotting (Fig. 1b). Due to superior stability of the knockdown effect over time, siRNA 2 was used in all following experiments.

First, we analyzed the effect of decreasing RECK biosynthesis to investigate whether endogenous RECK influences the expression of MMPs and TIMPs in hMSCs. RECK-deficient hMSCs showed no significant alteration in the transcription and biosynthesis of MMP-2, MT1-MMP and TIMP-1 compared to control cells (Fig. 1c–e). MMP-9 mRNA and protein were not detected either with or without RECK knockdown in hMSCs (data not shown). The mRNA levels of TIMP-2, however, were elevated in RECK-depleted cells 3 days after transfection consistent with an augmentation of TIMP-2 protein in 7 day-culture supernatants (Fig. 1f). These findings suggest that RECK promotes biosynthesis and release of TIMP-2 but has no influence on the expression of MMP-2, MT1-MMP, TIMP-1 and MMP-9 in hMSCs.

Importance of RECK in chemotactic migration of hMSCs

Next, we studied the role of endogenous RECK in hMSC migration using a scratch wound assay. Monolayers of hMSCs transfected with siRNA targeting RECK and control siRNA were subjected to scratch wounding and analyzed after 1, 2 and 3 days of incubation by microscopy. Wound closure was significantly faster in RECK-depleted hMSCs by comparison to control cells (Fig. 2a). Moreover, we used an Ibidi μ-Slide Chemotaxis³ᴰ assay to perform more detailed studies on RECK's role in directed migration of hMSC. Cells without and with RECK knockdown were tracked for 24 h. In the absence of chemoattractants, hMSCs showed solely random migration as confirmed by results of the Raleigh test (Table 1) and the moving direction (Fig. 2b, c; Table 1). In the presence of a chemotactic gradient formed by human serum, RECK-depleted hMSCs exhibited a higher chemotactic potential in comparison to cells transfected with control siRNA, as demonstrated by a lower Raleigh test probability value (Table 1) as well as increased values of moving direction (Fig. 2b, c; Table 1) and FMI (Table 1). In addition, hMSCs lacking RECK showed an enhanced migratory potential, as indicated by elevated values of the parameters COM (Fig. 2b; Table 1), migration distance (Fig. 2b, c; Table 1) and velocity (Table 1). Together, these findings provide evidence that endogenous RECK is an attenuator of directed migration in hMSCs.

Impact of RECK on hMSC differentiation and proliferation

We were interested whether expression of endogenous RECK was influenced upon differentiation of the cells
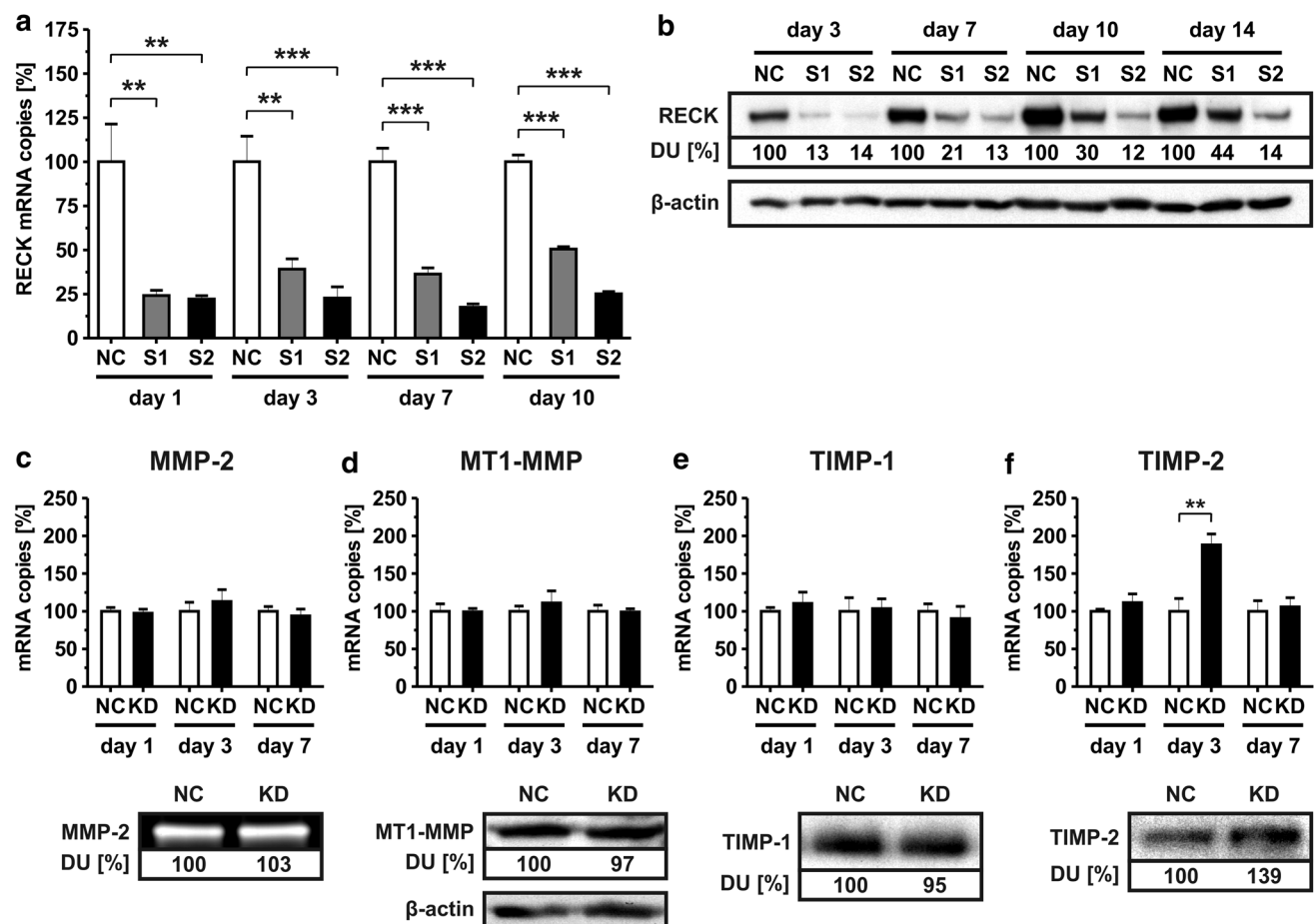
Fig. 1 Influence of RECK on MMP and TIMP expression in hMSCs. Cells were treated with control siRNA (NC) and two different siRNAs targeting RECK (S1, S2). **a** Relative mRNA expression of RECK was quantified by qRT-PCR analysis on day 1, 3, 7 and 10 after transfection and normalized to GAPDH mRNA. **b** Protein levels of RECK in cell extracts were determined by Western blotting on day 3, 7, 10 and 14 after transfection. For densitometric quantification, the amount of RECK present in cells transfected with control siRNA was set to 100 % at each time point. Cellular β-actin was used as a loading control. hMSCs were transfected with siRNA 2 (S2) against RECK (KD) and control siRNA (NC). Relative mRNA expression of MMP-2 (**c**), MT1-MMP (**d**), TIMP-1 (**e**) and TIMP-2 (**f**) was quantified by qRT-PCR analysis on day 1, 3 and 7 after transfection. Values were normalized to GAPDH mRNA. Protein levels of MMP-2 (**c**) as well as TIMP-1 (**e**) and TIMP-2 (**f**) were determined in supernatants after 7 days of cell cultivation analyzing equal amounts of protein by zymography and Western blotting, respectively. MT1-MMP (**d**) was detected in 7 day-cell extracts by Western blotting. Here, β-actin served as a loading control. Results of densitometric quantification are given in densitometric units (DU) with the amounts of protein present in control cells set as 100 %. Data shown represent the mean ± SD of triplicate measurements ($n = 3$). **$P < 0.01$; ***$P < 0.001$

into the adipogenic and osteogenic lineages. hMSCs incubated in adipogenic differentiation medium demonstrated reduced levels of RECK transcription whereas cells grown in osteogenic differentiation medium had significantly increased levels of RECK mRNA in comparison to control cells, when determined after both 3 and 14 days of cultivation (Fig. 3a). Consistently, RECK protein was diminished in hMSCs differentiated into the adipogenic lineage but augmented upon differentiation into osteogenic cells, as determined by Western blotting analysis after 3 and 14 days of incubation (Fig. 3b). To investigate whether endogenous RECK actively influences hMSC differentiation, cells transfected with siRNA against RECK or control siRNA were grown to subconfluency and cultivated in adipogenic and osteogenic differentiation media. After 10 days, quantification of mRNA expression in RECK-depleted hMSCs revealed higher levels of the adipogenic differentiation marker PPARγ and reduced quantities of the osteogenic differentiation marker ALP in comparison to control cells as determined by qRT-PCR (Fig. 3c). After 14 days, microscopic analysis of the Oil Red O-stained monolayers of cultivation demonstrated elevated numbers of lipid vacuoles in RECK-depleted cells compared to control cells (Fig. 3d). By contrast, the Alizarin Red S-stained monolayers showed decreased levels of mineralization in RECK knockdown cells in comparison to control cells (Fig. 3d). The results obtained by microscopy were
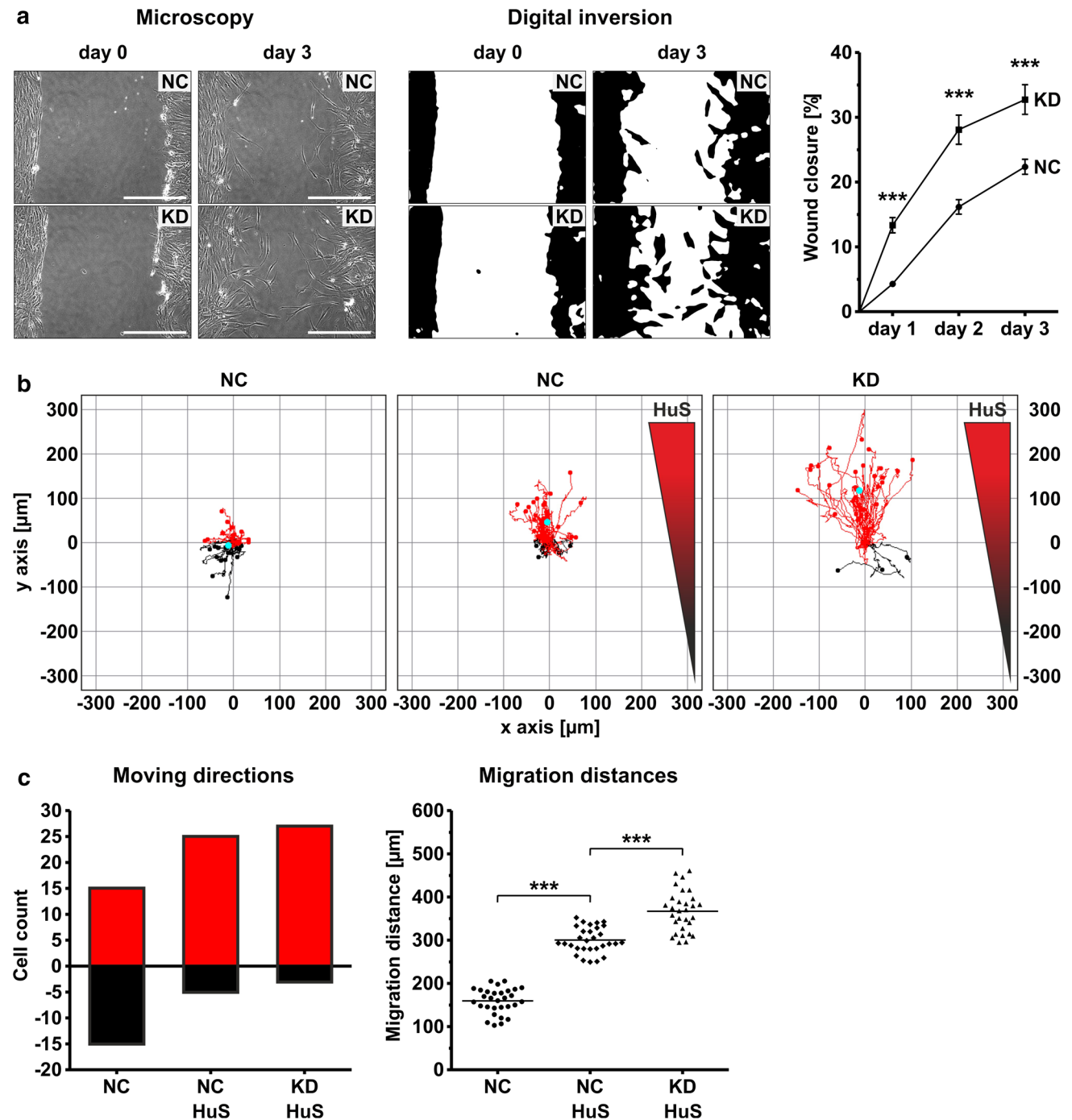
Fig. 2 RECK impairs the chemotaxis and migration potential in hMSCs. **a** Confluent monolayers of hMSCs transfected with siRNA targeting RECK (KD) and control siRNA (NC) were subjected to mechanical scratch wounding. The area covered by cells was recorded by phase-contrast microscopy connected to a digital camera at time 0 and after day 1, 2 and 3. *Scale bars* indicate 500 μm. The extent of wound closure in % was calculated by measuring the diminution of the area initially covered by cells over time adopting densitometric analysis of digitally inverted pictures using the ImageJ software. **b** Migration paths of hMSCs transfected with siRNA targeting RECK (KD) and control siRNA (NC) analyzed for 24 h in the absence and presence of human serum (HuS) as a chemoattractant using the Ibidi μ-Slide Chemotaxis^{3D} assay and Ibidi software. **c** Moving directions of 30 individual cells towards (*red*) and away from (*black*) the chemoattractant were quantified serving as a parameter of the chemotactic potential. Migration distances of 30 individual cells were determined serving as a parameter of the migratory potential. Data shown represent the mean ± SD of triplicate measurements ($n = 3$). ***$P < 0.001$

Table 1 Analysis of hMSC directed migration

hMSC	Chemotactic potential			Migratory potential		
	Rayleigh test (P)	Moving direction (towards/away)	FMI (x/y)	COM (x/y) (µm)	Migration distance (µm)	Velocity (µm/h)
NC	0.52	15/15	−0.057/−0.026	−10.82/−6.30	159.65	6.65
NC + HuS	1E−5	25/5	−0.023/0.154	−6.09/46.15	300.32	12.51
KD + HuS	1E−8	27/3	−0.038/0.314	−14.13/120.80	366.91	15.29

The chemotactic and migratory potential of hMSCs without (NC) and with RECK knockdown (KD) was studied using an Ibidi µ-Slide Chemotaxis^{3D} assay. At each experimental condition, 30 cells were tracked for 24 h in the absence and presence of human serum (HuS) as a chemoattractant and subsequently analyzed. Migration parameters shown in the table are defined in the "Materials and methods" section. Results shown are representative for three independent experiments
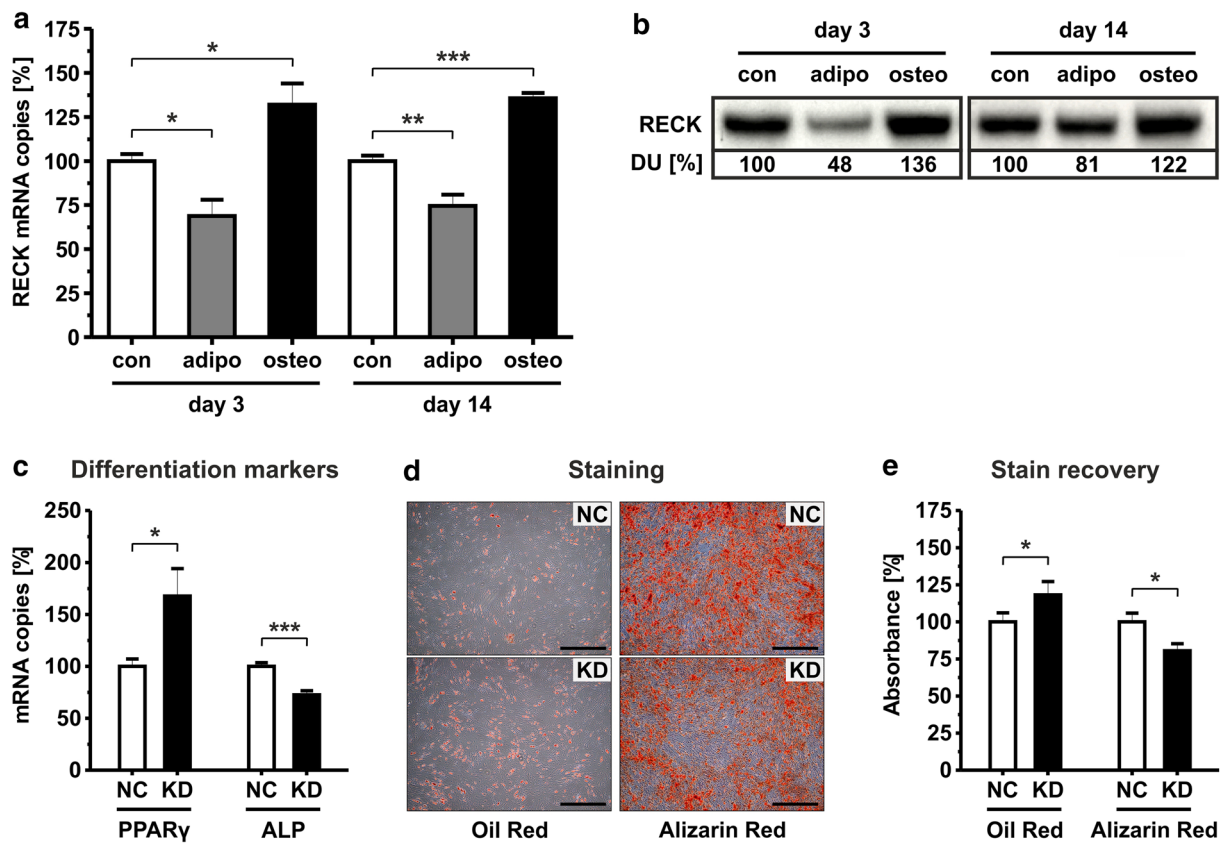

Fig. 3 RECK differentially controls adipogenesis and osteogenesis in hMSCs. hMSCs were cultivated for 3 and 14 days in the absence (con) and presence of adipogenic (adipo) and osteogenic (osteo) differentiation medium. **a** Relative transcriptional levels of RECK were quantified using qRT-PCR and normalized to GAPDH mRNA. **b** RECK present in cell extracts was determined by Western blot analysis applying equal amounts of total protein into each lane. Results of densitometric quantification are given in densitometric units (DU) with the amounts of protein present in control cells set as 100 %. hMSCs transfected with control siRNA (NC) or siRNA targeting RECK (KD) were incubated in adipogenic or osteogenic differentiation medium. **c** Relative mRNA expression of the differentiation markers PPARγ and ALP was quantified by qRT-PCR analysis after 10 days of differentiation. Values were normalized to GAPDH mRNA. Cell staining with Oil Red O for adipogenic and Alizarin Red S for osteogenic differentiation after 14 days of incubation in differentiation medium is shown by representative microscopic images of stained cellular monolayers (**d**) and stain recovery after extraction from the cells (**e**). *Scale bars* indicate 1 mm. Data shown represent the mean ± SD of triplicate measurements (n = 3). *P < 0.05; **P < 0.01; ***P < 0.001

confirmed through quantification of stain recovered via chemical elution from the Oil Red O- and Alizarin Red S-stained cells (Fig. 3e).

Studies on cell proliferation of hMSCs transfected with and without siRNA against RECK showed no differences in cell division rate and mitochondrial dehydrogenase

activity within 7 days of cultivation, as determined by the CyQuant cell proliferation assay and WST-8 assay, respectively (data not shown). Taken together, our findings demonstrate that expression of RECK in hMSCs has no influence on proliferation but differentially modulates adipogenic and osteogenic differentiation in these cells.

Influence of RECK on the Wnt/β-catenin signaling pathway

Because hMSC differentiation is essentially regulated by activity of Wnt/β-catenin signaling [21], we examined a potential impact of endogenous RECK on this pathway. The activation of the Wnt/β-catenin pathway is characterized by (a) the stabilization of cytoplasmic β-catenin, (b) the translocation of β-catenin into the nucleus followed by its interaction with TCF/LEF transcription factors and (c) the increased expression of β-catenin target genes. Therefore, we investigated each of these features experimentally. Western blot analysis revealed that β-catenin protein levels were reduced in hMSCs on day 7, 10 and 14 after RECK knockdown compared to control cells (Fig. 4a). We used a *Gaussia* luciferase-based reporter system to investigate the activation of β-catenin target promoters. This BAR system can be used to specifically monitor β-catenin activity on TCF/LEF-dependent gene transcription (e.g. *Gaussia* luciferase). hMSCs transfected with the BAR system (BAR-hMSCs) were treated with siRNA targeting RECK or control siRNA and cultivated for up to 14 days in the presence of Wnt3a to stimulate β-catenin activity. These studies revealed that β-catenin reporter activity was significantly reduced in hMSCs with impaired RECK biosynthesis relative to control cells over the 14-day period of measurement (Fig. 4b). To confirm the stimulatory effect of RECK on β-catenin-dependent signaling in hMSCs, we performed qRT-PCR analysis of the Wnt/β-catenin target genes *DKK1* [26], *AXIN2* [27] and *RUNX2* [28] which contain TCF/LEF binding sites in their promoter. RECK-deficient hMSCs demonstrated decreased transcription of *DKK1*, *AXIN2* and *RUNX2* compared to control cells after 14 days of incubation as determined by qRT-PCR (Fig. 4c). In summary, these results indicate that RECK is a positive regulator of Wnt/β-catenin signaling activity in hMSCs. Knockdown of β-catenin in hMSCs increased expression of PPARγ on mRNA and protein level 4 days after transfection (Fig. 4d–f), demonstrating that β-catenin activity negatively controls adipogenic differentiation in these cells.

Discussion

Our current study describes novel functions of RECK acting as an attenuator of migration, modulator of differentiation and stimulator of Wnt/β-catenin signaling in

hMSCs. RECK is widely studied for its role in cancer. In various tumor tissues, RECK deficiency correlates with increased levels of MMPs [37], tumor cell invasion and progression of the disease [33]. RECK blocks MMP-9 expression in tumor cells [30] by a so far unknown mechanism and inhibits MT1-MMP activity on the cell surface [32]. In hMSCs, RECK has no influence on the biosynthesis of MMP-9, MT1-MMP, MMP-2 and TIMP-1. Consistent with our data, RECK knockdown did not affect TIMP-1 expression in pituitary cells [48]. TIMP-2 production in hMSCs, however, is under negative control by endogenous RECK. In general, a lack of TIMP-2 on the cell surface impedes proMMP-2 activation by MT1-MMP with a negative impact on cell migration, as previously demonstrated by own studies in hMSCs [14]. In fact, RECK-depleted hMSCs with elevated TIMP-2 levels have increased migratory capabilities. Interestingly, TIMP-2 stimulates RECK expression in various cell types [49, 50], indicating the existence of a positive mutual feedback mechanism which controls the biosynthesis of RECK and TIMP-2 in cells. The inhibitory effect of RECK on hMSC migration may derive from various RECK-regulated gene products that are important in cellular motility such as proteases and their inhibitors, adhesion molecules, chemokine receptors as well as proteins of the cytoskeleton as previously demonstrated in glioma cells [51]. Involvement of multiple factors in RECK-controlled cell migration is confirmed by our finding that RECK attenuates not only the migratory but also the chemotactic potential in hMSCs. Further studies are warranted for the identification of RECK target genes in hMSCs affecting the directed migration of these cells.

RECK did not influence proliferation of hMSCs. This is in line with results obtained from certain tumor cells [36]. A positive regulatory effect of RECK on proliferation is reported from endothelial cells [52] and osteoarthritic chondrocytes [53] whereas negative influence of RECK on cell division is described in kidney cells [54] and various tumor cells [55, 56]. This indicates that RECK's influence on proliferation is diverse and cell type-specific.

RECK expression in hMSCs directly correlates with osteogenic differentiation of the cells. This agrees with previous studies by others providing solely correlative data in various cell types and animal models that suggested an implication of RECK in osteogenesis [57–60]. Our knockdown experiments demonstrate that RECK is a promoter of hMSC differentiation into osteoblasts. These findings may enhance the application of hMSCs for cell-based therapies to regenerate bone tissues under pathological conditions such as skeletal trauma and bone loss [8]. Moreover, RECK was shown to preserve bone mass by inhibition of osteoclast activity in osteosarcoma [55]. The influence of RECK in adipogenesis was not investigated so
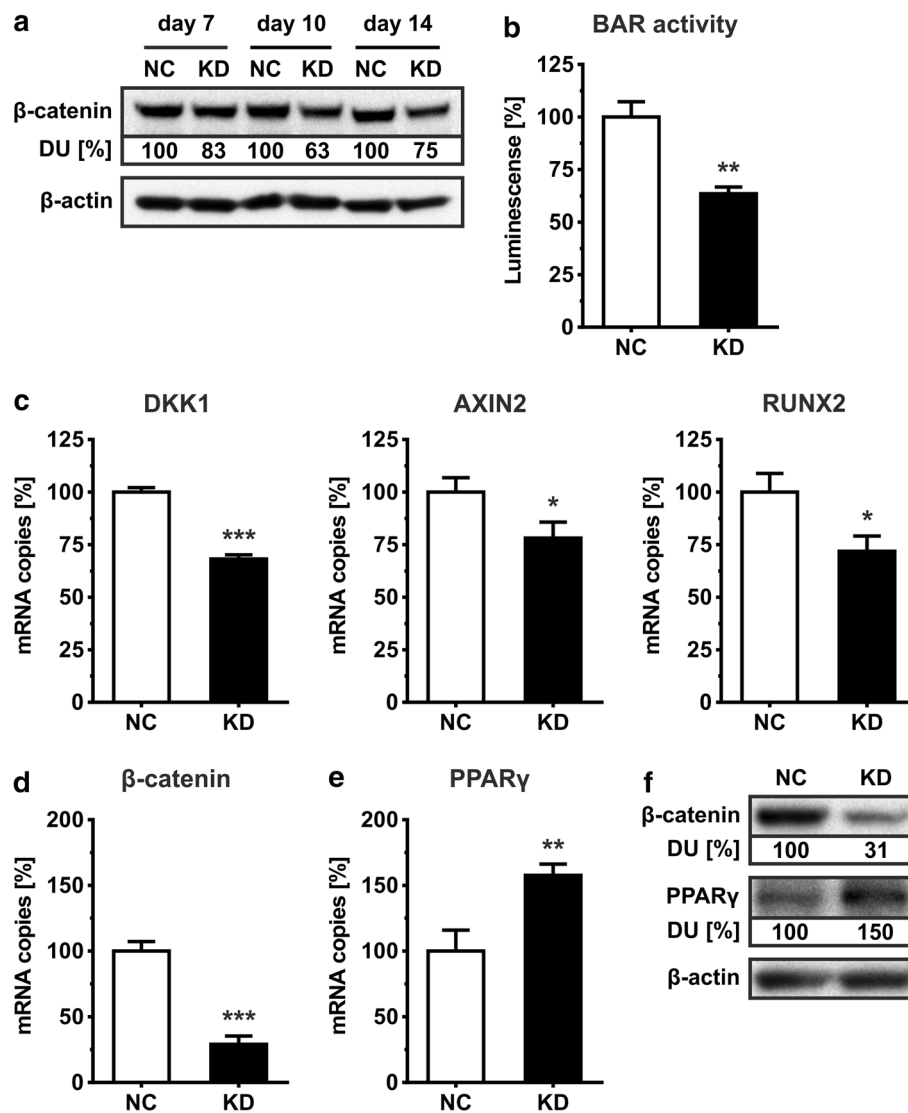
Fig. 4 RECK positively affects β-catenin stability and Wnt/β-catenin signaling activity. **a** Western blot analysis of β-catenin in protein extracts obtained from hMSCs transfected with siRNA against RECK (KD) and control siRNA (NC) on day 7, 10 and 14 after transfection. For densitometric quantification, protein levels are indicated in densitometric units (DU) with the amount of β-catenin present in control cells being set to 100 % at each time point. Cellular β-actin served as a loading control. **b** RECK knockdown (KD) and control hMSCs (NC) were transiently transfected with the BAR and further cultivated for 14 days. The activity of secreted *Gaussia* luciferase, which was transcribed due to β-catenin-dependent TCF/LEF signaling in the cells, was quantified in the conditioned medium. **c** Relative mRNA expression of the Wnt/β-catenin target genes *DKK1*, *AXIN2* and *RUNX2* was quantified by qRT-PCR analysis on day 10 after transfection. Effect of β-catenin knockdown on PPARγ expression. hMSCs were transfected with siRNA against β-catenin (KD) and control siRNA (NC) and analyzed on day 4 after transfection. **d** qRT-PCR analysis of β-catenin expression. **e** qRT-PCR analysis of PPARγ expression. **f** Western blot analysis of β-catenin and PPARγ in protein extracts. β-actin served as a loading control. All mRNA values were normalized to GAPDH mRNA. Experiments were performed in the absence (**a**) and presence (**b**, **c**) of recombinant Wnt3a. Data shown represent the mean ± SD of triplicate measurements ($n = 3$). *$P < 0.05$; **$P < 0.01$; ***$P < 0.001$

far. Our data for the first time provide evidence that RECK is a suppressor of adipogenic differentiation in hMSCs. Consistently, RECK expression is downregulated in these cells upon differentiation into adipocytes. Thus, our findings demonstrate reciprocal functions of RECK in hMSC lineage specification by acting as a stimulator of osteogenic differentiation and inhibitor of adipogenic differentiation in

these cells. A similar role in the control of these two processes in hMSCs is described for myocyte enhancer factor-2 [61]. This indicates that RECK among other factors is a master switch in the balance between osteogenesis and adipogenesis in hMSCs.

In search for underlying molecular mechanisms, we discovered that RECK is a positive effector of the Wnt/β-

catenin signaling pathway in hMSCs. This finding provides a plausible explanation of RECK's reciprocal function in osteogenic and adipogenic differentiation of hMSCs, because Wnt/β-catenin activity is reported by us and others to promote osteogenesis and to repress adipogenesis in these cells [42, 62, 63]. Consistently, knockdown of β-catenin in hMSCs increased PPARγ in these cells, further approving the attenuating role of the Wnt/β-catenin pathway in adipogenic differentiation of hMSCs. Moreover, we found RECK to upregulate the expression of RUNX2 in hMSCs. *RUNX2* is a target gene of Wnt/β-catenin signaling [28] and associated with osteoblast differentiation [64], confirming RECK's role as a stimulator of Wnt/β-catenin-triggered osteogenesis in these cells. Interestingly, further Wnt/β-catenin target genes, *DKK1* [26] and *AXIN2* [27], which are both upregulated by RECK in hMSCs are specific inhibitors of this pathway [65, 66]. This suggests that RECK contributes to a negative regulatory loop controlling the activity of Wnt/β-catenin signaling in hMSCs.

We have demonstrated that RECK is an attenuator of migration in hMSCs by mechanisms different from tumor cells. Furthermore, RECK acts as a master switch in the reciprocal control of osteogenic and adipogenic differentiation of hMSCs by promoting the former and blocking the latter. In addition, our results show that RECK is a positive effector of the Wnt/β-catenin signaling pathway which is involved in the regulation of various cell functions including migration and osteogenic differentiation. A deeper knowledge of RECK's role in hMSC biology may improve the development of novel therapeutic approaches to enhance bone formation during pathological bone loss.

Compliance with ethical standards

Conflict of interest The authors declare that they have no conflict of interest.

References

1. Horwitz EM, Le BK, Dominici M, Mueller I, Slaper-Cortenbach I, Marini FC, Deans RJ, Krause DS, Keating A (2005) Clarification of the nomenclature for MSC: The International Society for Cellular Therapy position statement. Cytotherapy. 7(5):393–395

2. Pittenger MF, Mackay AM, Beck SC, Jaiswal RK, Douglas R, Mosca JD, Moorman MA, Simonetti DW, Craig S, Marshak DR (1999) Multilineage potential of adult human mesenchymal stem cells. Science 284(5411):143–147

3. Egea V, von Baumgarten L, Schichor C, Berninger B, Popp T, Neth P, Goldbrunner R, Kienast Y, Winkler F, Jochum M, Ries C (2011) TNF-alpha respecifies human mesenchymal stem cells to a neural fate and promotes migration toward experimental glioma. Cell Death Differ 18(5):853–863

4. Jiang Y, Jahagirdar BN, Reinhardt RL, Schwartz RE, Keene CD, Ortiz-Gonzalez XR, Reyes M, Lenvik T, Lund T, Blackstad M, Du J, Aldrich S, Lisberg A, Low WC, Largaespada DA, Verfaillie CM (2002) Pluripotency of mesenchymal stem cells derived from adult marrow. Nature 418(6893):41–49

5. Mackenzie TC, Flake AW (2001) Human mesenchymal stem cells persist, demonstrate site-specific multipotential differentiation, and are present in sites of wound healing and tissue regeneration after transplantation into fetal sheep. Blood Cells Mol Dis 27(3):601–604

6. Wu GD, Nolta JA, Jin YS, Barr ML, Yu H, Starnes VA, Cramer DV (2003) Migration of mesenchymal stem cells to heart allografts during chronic rejection. Transplantation 75(5):679–685

7. Ryan JM, Barry F, Murphy JM, Mahon BP (2007) Interferon-gamma does not break, but promotes the immunosuppressive capacity of adult human mesenchymal stem cells. Clin Exp Immunol 149(2):353–363

8. Mankani MH, Kuznetsov SA, Wolfe RM, Marshall GW, Robey PG (2006) In vivo bone formation by human bone marrow stromal cells: reconstruction of the mouse calvarium and mandible. Stem Cells 24(9):2140–2149

9. Martens TP, Godier AF, Parks JJ, Wan LQ, Koeckert MS, Eng GM, Hudson BI, Sherman W, Vunjak-Novakovic G (2009) Percutaneous cell delivery into the heart using hydrogels polymerizing in situ. Cell Transplant 18(3):297–304

10. Zhao CP, Zhang C, Zhou SN, Xie YM, Wang YH, Huang H, Shang YC, Li WY, Zhou C, Yu MJ, Feng SW (2007) Human mesenchymal stromal cells ameliorate the phenotype of SOD1-G93A ALS mice. Cytotherapy 9(5):414–426

11. Fiorina P, Jurewicz M, Augello A, Vergani A, Dada S, La Rosa S, Selig M, Godwin J, Law K, Placidi C, Smith RN, Capella C, Rodig S, Adra CN, Atkinson M, Sayegh MH, Abdi R (2009) Immunomodulatory function of bone marrow-derived mesenchymal stem cells in experimental autoimmune type 1 diabetes. J Immunol 183(2):993–1004

12. Ringden O, Uzunel M, Rasmusson I, Remberger M, Sundberg B, Lonnies H, Marschall HU, Dlugosz A, Szakos A, Hassan Z, Omazic B, Aschan J, Barkholt L, Le Blanc K (2006) Mesenchymal stem cells for treatment of therapy-resistant graft-versus-host disease. Transplantation 81(10):1390–1397

13. Tanaka F, Tominaga K, Ochi M, Tanigawa T, Watanabe T, Fujiwara Y, Ohta K, Oshitani N, Higuchi K, Arakawa T (2008) Exogenous administration of mesenchymal stem cells ameliorates dextran sulfate sodium-induced colitis via anti-inflammatory action in damaged tissue in rats. Life Sci 83(23–24):771–779

14. Ries C, Egea V, Karow M, Kolb H, Jochum M, Neth P (2007) MMP-2, MT1-MMP, and TIMP-2 are essential for the invasive capacity of human mesenchymal stem cells: differential regulation by inflammatory cytokines. Blood 109(9):4055–4063

15. Malinowski M, Pietraszek K, Perreau C, Boguslawski M, Decot V, Stoltz JF, Vallar L, Niewiarowska J, Cierniewski C, Maquart FX, Wegrowski Y, Brezillon S (2012) Effect of lumican on the migration of human mesenchymal stem cells and endothelial progenitor cells: involvement of matrix metalloproteinase-14. PLoS ONE 7(12):e50709

16. Ponte AL, Ribeiro-Fleury T, Chabot V, Gouilleux F, Langonne A, Herault O, Charbord P, Domenech J (2012) Granulocyte-colony-stimulating factor stimulation of bone marrow mesenchymal stromal cells promotes CD34+ cell migration via a matrix metalloproteinase-2-dependent mechanism. Stem Cells Dev 21(17):3162–3172

17. Ho IA, Yulyana Y, Sia KC, Newman JP, Guo CM, Hui KM, Lam PY (2014) Matrix metalloproteinase-1-mediated mesenchymal stem cell tumor tropism is dependent on crosstalk with stromal derived growth factor 1/C-X-C chemokine receptor 4 axis. Faseb j 28(10):4359–4368

18. Olson MW, Gervasi DC, Mobashery S, Fridman R (1997) Kinetic analysis of the binding of human matrix metalloproteinase-2 and -9 to tissue inhibitor of metalloproteinase (TIMP)-1 and TIMP-2. J Biol Chem 272(47):29975–29983

19. Butler GS, Butler MJ, Atkinson SJ, Will H, Tamura T, Schade van Westrum S, Crabbe T, Clements J, d'Ortho MP, Murphy G (1998) The TIMP2 membrane type 1 metalloproteinase "receptor" regulates the concentration and efficient activation of progelatinase A. A kinetic study. J Biol Chem 273(2):871–880

20. Salazar KD, Lankford SM, Brody AR (2009) Mesenchymal stem cells produce Wnt isoforms and TGF-beta1 that mediate proliferation and procollagen expression by lung fibroblasts. Am J Physiol Lung Cell Mol Physiol 297(5):L1002–L1011

21. Qiu W, Andersen TE, Bollerslev J, Mandrup S, Abdallah BM, Kassem M (2007) Patients with high bone mass phenotype exhibit enhanced osteoblast differentiation and inhibition of adipogenesis of human mesenchymal stem cells. J Bone Miner Res 22(11):1720–1731

22. Neth P, Ciccarella M, Egea V, Hoelters J, Jochum M, Ries C (2006) Wnt signaling regulates the invasion capacity of human mesenchymal stem cells. Stem Cells 24(8):1892–1903

23. Mao J, Wang J, Liu B, Pan W, Farr GH 3rd, Flynn C, Yuan H, Takada S, Kimelman D, Li L, Wu D (2001) Low-density lipoprotein receptor-related protein-5 binds to Axin and regulates the canonical Wnt signaling pathway. Mol Cell 7(4):801–809

24. Molenaar M, van de Wetering M, Oosterwegel M, Peterson-Maduro J, Godsave S, Korinek V, Roose J, Destree O, Clevers H (1996) XTcf-3 transcription factor mediates beta-catenin-induced axis formation in Xenopus embryos. Cell 86(3):391–399

25. Behrens J, von Kries JP, Kuhl M, Bruhn L, Wedlich D, Grosschedl R, Birchmeier W (1996) Functional interaction of beta-catenin with the transcription factor LEF-1. Nature 382(6592):638–642

26. Niida A, Hiroko T, Kasai M, Furukawa Y, Nakamura Y, Suzuki Y, Sugano S, Akiyama T (2004) DKK1, a negative regulator of Wnt signaling, is a target of the beta-catenin/TCF pathway. Oncogene 23(52):8520–8526

27. Jho EH, Zhang T, Domon C, Joo CK, Freund JN, Costantini F (2002) Wnt/beta-catenin/Tcf signaling induces the transcription of Axin2, a negative regulator of the signaling pathway. Mol Cell Biol 22(4):1172–1183

28. Gaur T, Lengner CJ, Hovhannisyan H, Bhat RA, Bodine PV, Komm BS, Javed A, van Wijnen AJ, Stein JL, Stein GS, Lian JB (2005) Canonical WNT signaling promotes osteogenesis by directly stimulating Runx2 gene expression. J Biol Chem 280(39):33132–33140

29. Takahashi C, Sheng Z, Horan TP, Kitayama H, Maki M, Hitomi K, Kitaura Y, Takai S, Sasahara RM, Horimoto A, Ikawa Y, Ratzkin BJ, Arakawa T, Noda M (1998) Regulation of matrix metalloproteinase-9 and inhibition of tumor invasion by the membrane-anchored glycoprotein RECK. Proc Natl Acad Sci U S A 95(22):13221–13226

30. Takagi S, Simizu S, Osada H (2009) RECK negatively regulates matrix metalloproteinase-9 transcription. Cancer Res 69(4):1502–1508

31. Oh J, Takahashi R, Kondo S, Mizoguchi A, Adachi E, Sasahara RM, Nishimura S, Imamura Y, Kitayama H, Alexander DB, Ide C, Horan TP, Arakawa T, Yoshida H, Nishikawa S, Itoh Y, Seiki M, Itohara S, Takahashi C, Noda M (2001) The membrane-anchored MMP inhibitor RECK is a key regulator of extracellular matrix integrity and angiogenesis. Cell 107(6):789–800

32. Miki T, Takegami Y, Okawa K, Muraguchi T, Noda M, Takahashi C (2007) The reversion-inducing cysteine-rich protein with Kazal motifs (RECK) interacts with membrane type 1 matrix metalloproteinase and CD13/aminopeptidase N and modulates their endocytic pathways. J Biol Chem 282(16):12341–12352

33. Namwat N, Puetkasichonpasutha J, Loilome W, Yongvanit P, Techasen A, Puapairoj A, Sripa B, Tassaneeyakul W, Khuntikeo N, Wongkham S (2011) Downregulation of reversion-inducing-cysteine-rich protein with Kazal motifs (RECK) is associated with enhanced expression of matrix metalloproteinases and cholangiocarcinoma metastases. J Gastroenterol 46(5):664–675

34. Bergers G, Brekken R, McMahon G, Vu TH, Itoh T, Tamaki K, Tanzawa K, Thorpe P, Itohara S, Werb Z, Hanahan D (2000) Matrix metalloproteinase-9 triggers the angiogenic switch during carcinogenesis. Nat Cell Biol 2(10):737–744

35. Guo H, Li Q, Li W, Zheng T, Zhao S, Liu Z (2014) MiR-96 downregulates RECK to promote growth and motility of non-small cell lung cancer cells. Mol Cell Biochem 390(1–2):155–160

36. Walsh LA, Roy DM, Reyngold M, Giri D, Snyder A, Turcan S, Badwe CR, Lyman J, Bromberg J, King TA, Chan TA (2014) RECK controls breast cancer metastasis by modulating a convergent, STAT3-dependent neoangiogenic switch. Oncogene 34(17):2189–2203

37. Jacomasso T, Trombetta-Lima M, Sogayar MC, Winnischofer SM (2014) Downregulation of reversion-inducing cysteine-rich protein with Kazal motifs in malignant melanoma: inverse correlation with membrane-type 1-matrix metalloproteinase and tissue inhibitor of metalloproteinase 2. Melanoma Res 24(1):32–39

38. Hoelters J, Ciccarella M, Drechsel M, Geissler C, Gulkan H, Bocker W, Schieker M, Jochum M, Neth P (2005) Nonviral genetic modification mediates effective transgene expression and functional RNA interference in human mesenchymal stem cells. J Gene Med 7(6):718–728

39. Reynolds A, Leake D, Boese Q, Scaringe S, Marshall WS, Khvorova A (2004) Rational siRNA design for RNA interference. Nat Biotechnol 22(3):326–330

40. Naumann K, Wehner R, Schwarze A, Petzold C, Schmitz M, Rohayem J (2013) Activation of dendritic cells by the novel Toll-like receptor 3 agonist RGC100. Clin Dev Immunol 2013:283649

41. Nolte A, Ott K, Rohayem J, Walker T, Schlensak C, Wendel HP (2013) Modification of small interfering RNAs to prevent off-target effects by the sense strand. N Biotechnol 30(2):159–165

42. Egea V, Zahler S, Rieth N, Neth P, Popp T, Kehe K, Jochum M, Ries C (2012) Tissue inhibitor of metalloproteinase-1 (TIMP-1) regulates mesenchymal stem cells through let-7f microRNA and Wnt/beta-catenin signaling. Proc Natl Acad Sci USA 109(6):E309–E316

43. Biechele TL, Adams AM, Moon RT (2009) Transcription-based reporters of Wnt/beta-catenin signaling. Cold Spring Harb Protoc 2009(6):pdb prot5223

44. Ries C, Pitsch T, Mentele R, Zahler S, Egea V, Nagase H, Jochum M (2007) Identification of a novel 82 kDa proMMP-9 species associated with the surface of leukaemic cells: (auto-)catalytic activation and resistance to inhibition by TIMP-1. Biochem J 405(3):547–558

45. Lipton A, Klinger I, Paul D, Holley RW (1971) Migration of mouse 3T3 fibroblasts in response to a serum factor. Proc Natl Acad Sci USA 68(11):2799–2801

46. Heggebo J, Haasters F, Polzer H, Schwarz C, Saller MM, Mutschler W, Schieker M, Prall WC (2014) Aged human mesenchymal stem cells: the duration of bone morphogenetic protein-2 stimulation determines induction or inhibition of osteogenic differentiation. Orthop Rev (Pavia) 6(2):5242

47. Rayleigh L (1919) XXXI. On the problem of random vibrations, and of random flights in one, two, or three dimensions. Philosophical Magazine Series 6 37(220):321–347

48. Yoshida D, Nomura R, Teramoto A (2008) Regulation of cell invasion and signalling pathways in the pituitary adenoma cell line, HP-75, by reversion-inducing cysteine-rich protein with kazal motifs (RECK). J Neurooncol 89(2):141–150

49. Oh J, Seo DW, Diaz T, Wei B, Ward Y, Ray JM, Morioka Y, Shi S, Kitayama H, Takahashi C, Noda M, Stetler-Stevenson WG (2004) Tissue inhibitors of metalloproteinase 2 inhibits endothelial cell migration through increased expression of RECK. Cancer Res 64(24):9062–9069

50. Oh J, Diaz T, Wei B, Chang H, Noda M, Stetler-Stevenson WG (2006) TIMP-2 upregulates RECK expression via dephosphorylation of paxillin tyrosine residues 31 and 118. Oncogene 25(30):4230–4234

51. Silveira Correa TC, Massaro RR, Brohem CA, Taboga SR, Lamers ML, Santos MF, Maria-Engler SS (2010) RECK-mediated inhibition of glioma migration and invasion. J Cell Biochem 110(1):52–61

52. Miki T, Shamma A, Kitajima S, Takegami Y, Noda M, Nakashima Y, Watanabe K, Takahashi C (2010) The ss1-integrin-dependent function of RECK in physiologic and tumor angiogenesis. Mol Cancer Res 8(5):665–676

53. Kimura T, Okada A, Yatabe T, Okubo M, Toyama Y, Noda M, Okada Y (2010) RECK is up-regulated and involved in chondrocyte cloning in human osteoarthritic cartilage. Am J Pathol 176(6):2858–2867

54. Lee YM, Lee SH, Lee KB, Nguyen MP, Lee MY, Park GH, Kwon MJ (2013) Silencing of reversion-inducing cysteine-rich protein with Kazal motifs stimulates hyperplastic phenotypes through activation of epidermal growth factor receptor and hypoxia-inducible factor-2alpha. PLoS ONE 8(12):e84520

55. Clark JC, Akiyama T, Thomas DM, Labrinidis A, Evdokiou A, Galloway SJ, Kim HS, Dass CR, Choong PF (2011) RECK in osteosarcoma: a novel role in tumour vasculature and inhibition of tumorigenesis in an orthotopic model. Cancer 117(15):3517–3528

56. Yoshida Y, Ninomiya K, Hamada H, Noda M (2012) Involvement of the SKP2-p27(KIP1) pathway in suppression of cancer cell proliferation by RECK. Oncogene 31(37):4128–4138

57. Accorsi-Mendonca T, Paiva KB, Zambuzzi WF, Cestari TM, Lara VS, Sogayar MC, Taga R, Granjeiro JM (2008) Expression of matrix metalloproteinases-2 and -9 and RECK during alveolar bone regeneration in rat. J Mol Histol 39(2):201–208

58. Zambuzzi WF, Yano CL, Cavagis AD, Peppelenbosch MP, Granjeiro JM, Ferreira CV (2009) Ascorbate-induced osteoblast differentiation recruits distinct MMP-inhibitors: RECK and TIMP-2. Mol Cell Biochem 322(1–2):143–150

59. Visigalli D, Strangio A, Palmieri D, Manduca P (2010) Hind limb unloading of mice modulates gene expression at the protein and mRNA level in mesenchymal bone cells. BMC Musculoskelet Disord 11:147

60. Alexander D, Ardjomandi N, Munz A, Friedrich B, Reinert S (2011) ECM remodelling components regulated during jaw periosteal cell osteogenesis. Cell Biol Int 35(10):973–980

61. Chen YH, Yeh FL, Yeh SP, Ma HT, Hung SC, Hung MC, Li LY (2011) Myocyte enhancer factor-2 interacting transcriptional repressor (MITR) is a switch that promotes osteogenesis and inhibits adipogenesis of mesenchymal stem cells by inactivating peroxisome proliferator-activated receptor gamma-2. J Biol Chem 286(12):10671–10680

62. D'Alimonte I, Lannutti A, Pipino C, Di Tomo P, Pierdomenico L, Cianci E, Antonucci I, Marchisio M, Romano M, Stuppia L, Caciagli F, Pandolfi A, Ciccarelli R (2013) Wnt signaling behaves as a "master regulator" in the osteogenic and adipogenic commitment of human amniotic fluid mesenchymal stem cells. Stem Cell Rev 9(5):642–654

63. Gattu AK, Swenson ES, Iwakiri Y, Samuel VT, Troiano N, Berry R, Church CD, Rodeheffer MS, Carpenter TO, Chung C (2013) Determination of mesenchymal stem cell fate by pigment epithelium-derived factor (PEDF) results in increased adiposity and reduced bone mineral content. FASEB J 27(11):4384–4394

64. Ducy P, Zhang R, Geoffroy V, Ridall AL, Karsenty G (1997) Osf2/Cbfa1: a transcriptional activator of osteoblast differentiation. Cell 89(5):747–754

65. Fedi P, Bafico A, Nieto Soria A, Burgess WH, Miki T, Bottaro DP, Kraus MH, Aaronson SA (1999) Isolation and biochemical characterization of the human Dkk-1 homologue, a novel inhibitor of mammalian Wnt signaling. J Biol Chem 274(27):19465–19472

66. Behrens J, Jerchow BA, Wurtele M, Grimm J, Asbrand C, Wirtz R, Kuhl M, Wedlich D, Birchmeier W (1998) Functional interaction of an axin homolog, conductin, with beta-catenin, APC, and GSK3beta. Science 280(5363):596–599